

Dissertation Abstract

可変ピッチ翼を有する小形垂直軸風車の数値及び実験的研究

Numerical and Experimental Studies of a Small Vertical-Axis Wind Turbine with Variable-Pitch Blades

Graduate School of Natural Science & Technology
Kanazawa University

Rachmat Firdaus

Major subject:

Division of Innovative of Science and Technology

Course: Fluid Dynamic

Abstract

This thesis presents numerical simulations and experiments on the effect of the variable pitch angle of blade rotor on the performance of small vertical-axis wind turbines (Darrieus and Orthopter wind turbine). The power, torque, and flow around blade rotor of VAWTS were analyzed by two-dimensional unsteady computational fluid dynamics simulations using ANSYS Fluent 13.0 program. The Darrieus rotor was composed using three NACA0018 airfoil straight blades. Three different rotor blade configurations were employed which i.e., a fixed-pitch blade with a pitch angle, variable blade pitch angle. The Orthopter rotor blades rotate movement around its own axis a half relative to the main rotor in one revolution. The configurations of different aspect ratio and number of blade (of the Orthopter rotor blade) were employed.

The effects of the variable-pitch angle, tip speed ratio, and three turbulent models, i.e., the RNG $k-\varepsilon$, Realizable $k-\varepsilon$, and SST $k-\omega$ turbulent models, on the performance of Darrieus wind turbine were investigated. The effect of number of blades, tip speed ratio, and aspect ratio of the Orthopter wind turbine with flat-plate blades rotor were also investigated by numerical simulation using RNG $k-\varepsilon$ turbulent model. The result predictions of numerical were validated by open circuit wind tunnel experimental data.

The numerical simulations results of both a VAWT with variable pitch blade and the orthopter wind turbine had good qualitative agreement with the experiments results. The predictions of performance of using the RNG $k-\varepsilon$ turbulence model were very close with experimental data. The VAWT with variable-pitch blades has better performance than a VAWT with fixed-pitch blades and by RNG $k-\varepsilon$ and SST $k-\omega$ turbulent models, its can suppress the occurrence of a vortex on its blades at a low tip speed ratio. The performance of the Orthopter is influenced by aspect ratio, number of blade, and tip speed ratio. The highest performance of Orthopter wind turbine at $AR=1$. The high tip speed ratio lead to reducing torque generation especially at downstream area. The simulations show effects of number of blade on the performance. The high number of blade reduces torque generation of one blade. However, the overall of performance was increased.

Introduction

1.1 Background

Recently, the world market for small wind turbine has seen further strength growth and common applications of one include; residential, hybrid system, fishery, commercial and industrial. Total installed wind turbine capacity more than 400000MW in 2014 (WWEA 2013).

The wind turbine can be classified into two categories. The first is the orientation of the rotation axis of the turbine (parallel or transverse to the wind flow) which i.e. vertical axis wind turbine (VAWT) and horizontal axis wind turbine (HAWT). The second is the methods of power generation source which i.e. wind turbines are called lift-based or drag-based. The Darrieus, Savonius, and Orthopter wind turbine are vertical axis wind turbine.

Generally, HAWTs have higher efficiency than all VAWTs followed by Darrieus turbine (lift-based type) and Savonius turbine (drag-based type). However, VAWTs have many advantages, such as being omni-directional without needing a yaw control system, having better aesthetics for their integration into buildings, and having lower sound emissions; therefore, VAWTs are expected to be used in urban areas.

Torque generation of rotor blade of Darrieus and Drag-type turbine are vary correspondent to azimuth position. Positive torque of Darrieus turbine mostly generate at upstream area and decreasing power generation at downstream area due to wake effect. The drag-type turbine has positive torque generation at advising blade position or lower side wind area. The drawback of drag-type turbine is negative power in upper wind area due to reverse force on the returning blade. The dynamic stall phenomenon, which is a major component of the unsteady aerodynamics of a Darrieus wind turbine at low tip speed ratio contribute on the drawback of turbine.

Therefore, modified of pitch angle rotor blades of WAVTs are needed to overcome turbine disadvantages. There are two types of modifications, the first type is Darrieus wind turbine with variable pitch, and the second type is the Orthopter wind turbine. The orthopter wind turbine is combination between a drag-type and a lift-type vertical axis wind turbine. The blade rotor of Orthopter wind turbine enable rotating its own axis and turbine's shaft axis as simultaneously

1.2 Objectives

To improve the performance and aerodynamic behaviour of both wind turbines were investigated by numerical studies using ANSYS Fluent 13.0 programs. The predictions of performances were validated by open circuit wind tunnel testing. The effect of variable pitch angle blade of Darrieus wind turbine and the effect number blade and aspect ratio of rotor of the orthopter wind turbine were also investigated.

2. Methodology

2.1 Wind turbine parameters

Wind velocity or free-stream velocity (V_{∞}) is uniform flow speed of wind. Induced velocity (V_i) is inlet velocity of the rotor blade, it depends on wake condition. The vertical axis wind turbine has difference of inlet velocity between upstream and downstream area. Tangential velocity is velocity of turbine blade rotor given by the angular velocity times the radius of rotor wind turbine ($V_t = \omega \cdot R$). Relative velocity (W) is sum of vector velocity of inlet velocity and tangential velocity ($W = V_i + V_t$).

Tip speed ratio (λ) define ratio tangential velocity of blade rotor to free-stream velocity ($\lambda = V_t / V_{\infty}$). Aspect ratio (AR) define ratio chord length of blade to length of span blade ($AR = C/L$). Solidity (σ) define ratio of total blade area to circumference area for VAWT and swept area for HAWT ($\sigma = n \cdot C / A$). Swept area (A) equals the

projected frontal area of the wind turbine given by the height of rotor times the diameter of the rotor ($A = L \cdot D$) for the VAWT and ($A = \pi R^2$) for the HAWT

The power coefficient (C_P) is performance of wind turbine. This coefficient represents ratio the produced energy of the wind turbine to the total wind energy passing through the swept area of the wind turbine. This coefficient is normally plotted against the tip speed ratio λ at a certain free-stream velocity or Reynolds number based on diameter rotor or chord length blade.

$$C_P = \frac{P}{\rho A V^3}$$

$$P = T \cdot \omega$$

T = torque of rotor shaft wind turbine (measured by torque transducer)

ω = rotational speed of rotor shaft wind turbine

C_T = Torque coefficient

$$C_T = \frac{T}{\rho A V^2}$$

2.2 Model geometry

There are two types modified wind turbine which i.e., the Darrieus with variable pitch angle rotor blade and the orthopter wind turbine. The main geometrical features of Darrieus wind turbine with variable pitch angle blade are shown in Figure 1a. The rotor diameter and height of wind turbine are $D (=2R) = 800$ mm and $h = 800$ mm respectively. The section of the VAWT that was analyzed was the symmetrical airfoil of its NACA0018 blade. The rotor of the VAWT was composed of three blades with a chord length of $c = 200$ mm and a main shaft with a diameter of 0.06 m. Figure 1b shows the top view of a variable pitch of VAWT. The variable-pitch mechanism consists of an adjustable four-bar linkage.

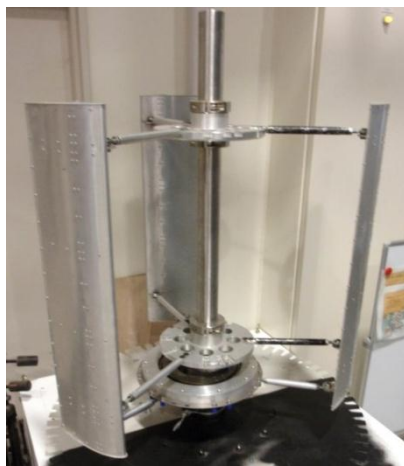


Fig. 1a Vertical axis wind turbine with variable-pitch straight blades

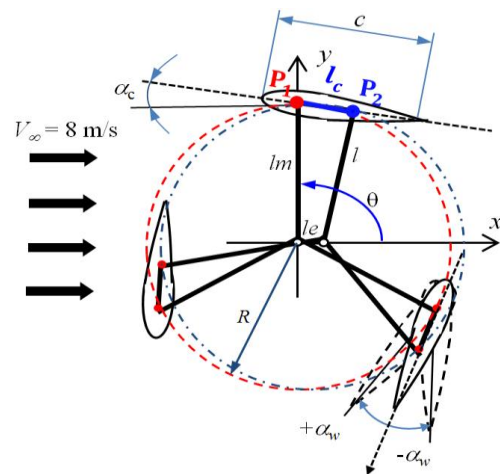


Fig. 1b A variable- pitch blade rotor mechanism with a four- bar linkage

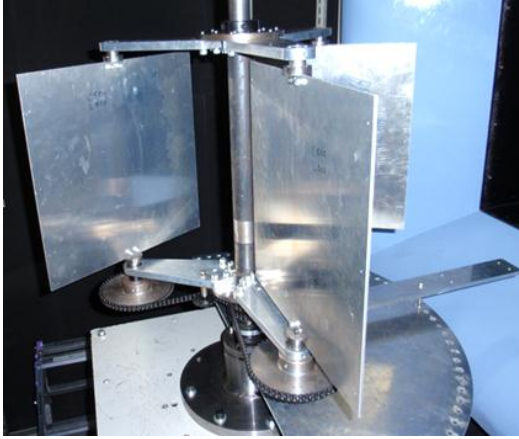


Fig. 2a Orthopter wind turbine with 3 flat plate blades

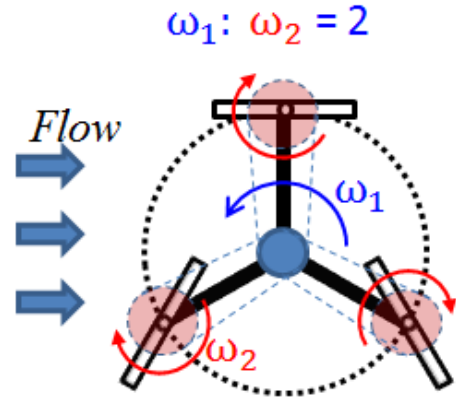


Fig. 2b Schematic blades rotation on orthopter wind turbine

Blade pitch angle vary by adjustable eccentric link (l_e) that has an eccentric rotational point O_e that is different from the main rotational point O . Point P_1 is near the leading edge of the blade, and point P_2 is near the trailing edge of the blade. The angle between the main-link (l_m) and the eccentric-link (l_e) is the azimuth angle (θ).

Figures 2a and 2b show the schematic of orthopter wind turbine. The orthopter composed of 2, 3, and 4 blades with different aspect ratio. The pitch of the blades was controlled by using a chain and sprockets arrangement to ensure that the blades rotated around their own axis by 360 degrees during the each two full revolution of the main rotor. The orthopter wind turbine had rotor diameter $D = 510\text{mm}$ with chord blade $c = 225\text{mm}$, $c = 298\text{mm}$, and $c=400\text{ mm}$ for aspects ratio $AR = 2$, $AR = 1.5$, and $AR = 1$ respectively.

2.3 Experimental set up

Figure 3 shows a schematic diagram of the experimental apparatus. The experiments were carried out in open circuit wind tunnel to reduce blockage effect with test-section dimension had a cross-sectional area of $1250\text{ mm} \times 1250\text{ mm}$. The uniform flow in the

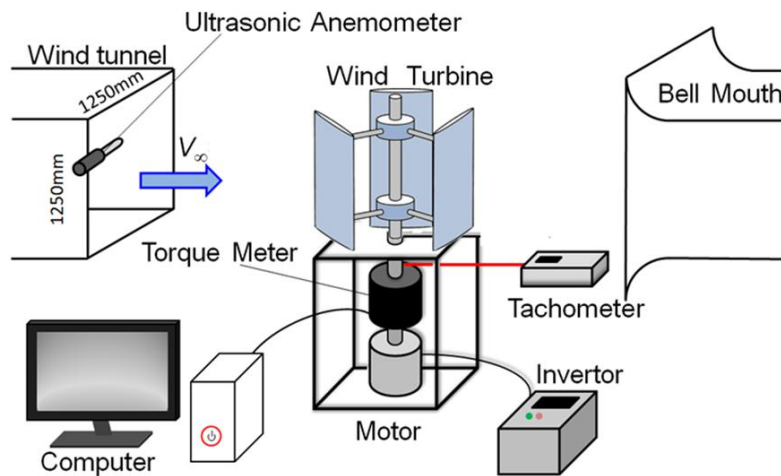


Fig. 3 Schematic diagrams of experimental apparatus

analyzed area was measured by an ultrasonic anemometer. The turbulence and non-uniform level variation in the exit of nozzle at a wind speed

$V_\infty = 8 \text{ m/s}$ was less than 0.5% and $\pm 1.0\%$, respectively. A geared motor and a frequency inverter with aerodynamic breaking resistor were used to drive the wind turbine. The torque T and rotation speed N of the wind turbine were measured in each case in order to calculate the power coefficient $C_P (= T\omega/0.5\rho D h V_\infty^3; \rho, \text{ air density; } \omega, \text{ turbine angular velocity})$ by using a torque transducer and a digital tachometer under a constant wind velocity of $V_\infty = 8 \text{ m/s}$.

2.4 Numerical simulation

The two-dimensional computational domain, the boundary conditions and the mesh structure are shown in figure 4 for Darrieus wind turbine and figure 5 for the orthopter wind turbine. The computational domain had a radius of $24R$ and $40R$ for Darrieus and orthopter wind turbine respectively. The inlet and outlet boundary conditions were placed respectively upstream and downstream of the rotor as shown in Figs. 4 and 5. The inlet of the computational domain corresponded to the uniform flow condition at $V_\infty = 8 \text{ m/s}$ and $V_\infty = 10 \text{ m/s}$ for Darrieus and orthopter wind turbine respectively with a turbulence intensity of 1.0% and turbulence viscosity ratio of 5 %. The pressure outlet condition for $\Delta p = 0$ was specified at the downstream boundaries of the computational. The Darrieus and orthopter wind turbine had three mesh domains with total number of elements was about 3.37×10^5 and 9.7×10^4 respectively. The governing equations were the continuity equation and the unsteady Reynolds-averaged Navier-Stokes (URANS) equation, in which the Reynolds stresses were solved by using the three different turbulence models (the RNG $k-\varepsilon$, Realizable $k-\varepsilon$, and SST $k-\omega$ models) for Darrieus wind turbine. The implicit algorithm of the PISO method was applied for the pressure-velocity coupling

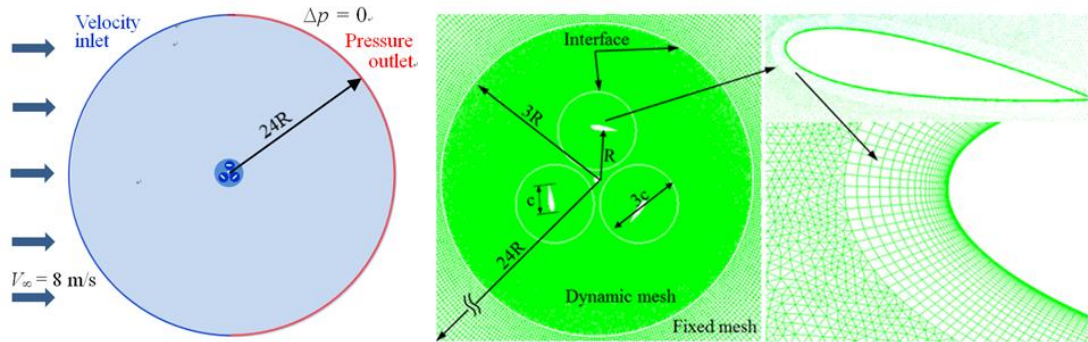


Fig. 4 Computational domain and boundary conditions of Darrieus wind turbine

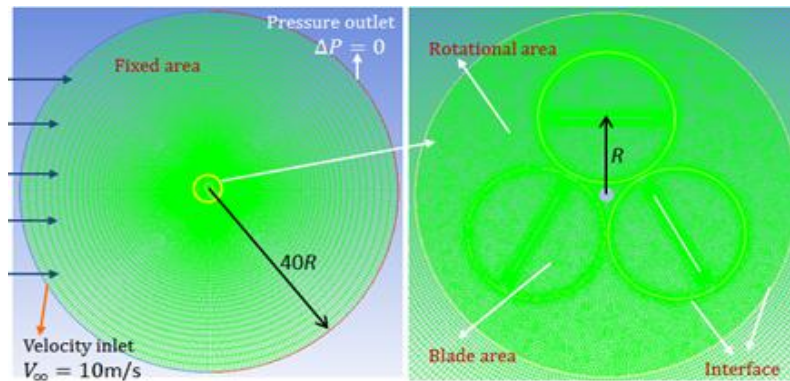


Fig. 5 Computational domain and boundary conditions of Orthopter wind turbine

3. Result

3.1 Darrieus wind turbine with fixed- and variable pitch blades

3.1.1 Effect of variable pitch angle on power coefficients

The power coefficients C_p of the VAWTs with variable- and fixed-pitch blades for the numerical simulation and experiment are shown in Figs. 6a and 6b, respectively. These figures present the effects of the blade pitch angle amplitude α_w on the power coefficient of the wind turbine. The effects of the blade pitch angle amplitude qualitatively agree with the two-dimensional numerical simulation using the RNG $k-\varepsilon$ turbulence model and the experiment. The power coefficient of the VAWT with variable-pitch blades of $\alpha_w = \pm 10.2^\circ$ is higher than that with fixed-pitch blades. The peak power coefficients of the variable-pitch blades with $\alpha_w = \pm 10.2^\circ$ and the fixed-pitch blades occur at a higher TSR as compared to those with variable-pitch blades with $\alpha_w = \pm 15.0^\circ$.

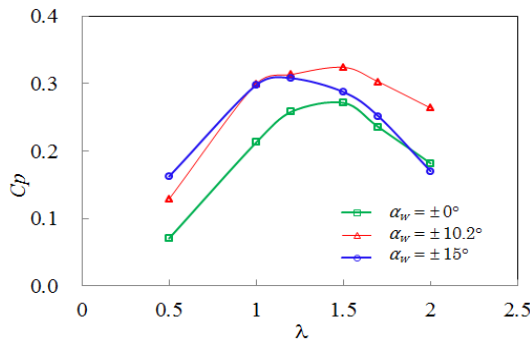


Fig. 6a Numerical result of power performance

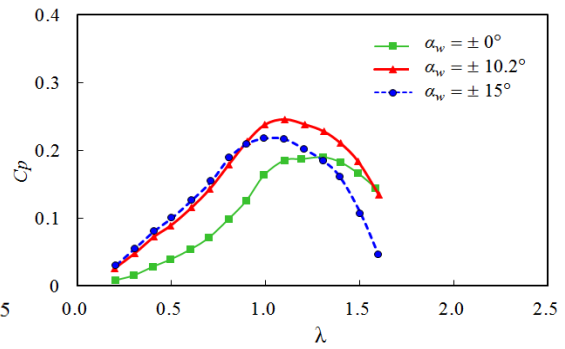


Fig. 6b Experiment result of power performance

3.1.2 Effect of tip speed ratio on torque coefficients

The power and torque coefficients of the VAWT with variable-pitch blades of $\alpha_w = \pm 10.2^\circ$ is shown in Fig. 7a. Total power and torque coefficients are divided into two components in the upstream and downstream areas. The power coefficient in the upstream area increases as the tip speed ratio (TSR) increase. However, the total power coefficient was increase until TSR of $\lambda = 1.5$, then decrease as the power coefficient in the downstream area decrease. The torque coefficient for $\lambda \leq 1.5$ is positive in both upstream and downstream areas (Curves C_{TU} and C_{TD}). However, for $\lambda > 1.5$, the torque coefficient in the downstream area becomes negative, and the torque coefficient decreases with an increase in the TSR. The total torque coefficient (Curve C_{TT}) increases until TSR of $\lambda = 1.0$, then decrease due to the decrement of torque coefficient in both upstream and downstream areas.

Figure 7b shows the effects of the TSR on the torque coefficient $C_{TBK}(\theta)$ for one cycle of the variable-pitch blades with $\alpha_w = \pm 10.2^\circ$. The torque coefficient fluctuations of one blade at four different tip speed ratio are presented in this figure. For low TSR of $\lambda = 0.5$, the maximum torque coefficient is generated at $\theta \approx 180^\circ$, and the torque coefficient is almost positive at all azimuth angles (except $90^\circ < \theta < 125^\circ$ as the inside circle a). The maximum value and peak angle of torque coefficient varies with tip speed ratios (shown as the inside of circle b in Fig. 7b). For low tip speed ratio ($\lambda = 0.5$), the maximum value of torque coefficient has higher than one for high tip speed ratio and shifted to large azimuth angle with increasing the tip speed ratio. The azimuth angle for the maximum torque coefficient increases with an increase in the TSR. The shift of the azimuthal angle for the maximum torque coefficient relates the angle of attack of the

rotating blade, i.e. the azimuthal angle where the angle of attack becomes the maximum lift coefficient ($\alpha \approx 15^\circ$) or the minimum angle of attack.

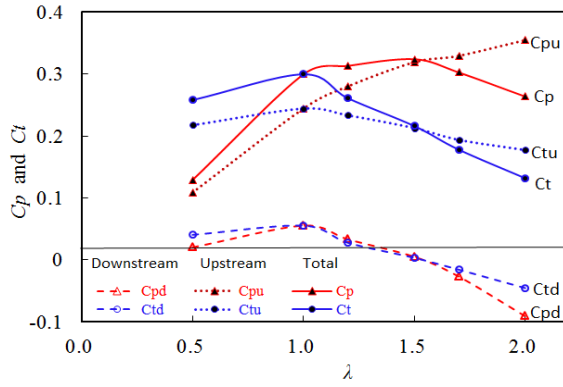


Fig. 7a Effects tip speed ratio on the performance

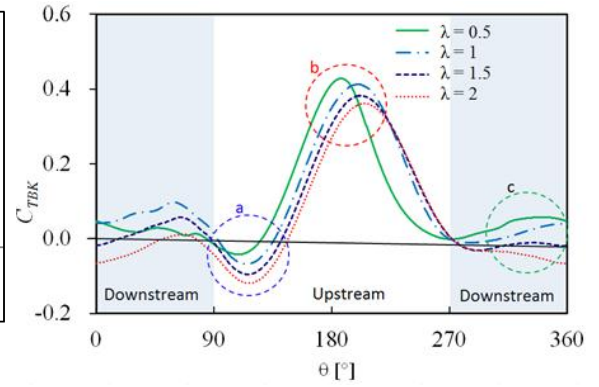


Fig. 7b Effects tip speed ratio on C_T in one blade

3.1.3 Dynamic stall on a blade

Figures 8 and 9 show the vorticity contours around the VAWT with fixed- and variable-pitch blades with $\alpha_w = \pm 10.2^\circ$ at an operating TSR of $\lambda = 1.0, 1.5$, and 2.0 using the SST $k-\omega$ model and RNG $k-\varepsilon$ model respectively. The presence of vortex on blade occurred on both fixed- and variable pitch blade at low tip speed ratio. Figure 8(a) and 9(b) show the absence of a vortex at a TSR of $\lambda = 1.5$ on variable-pitch blades with $\alpha_w = \pm 10.2^\circ$.

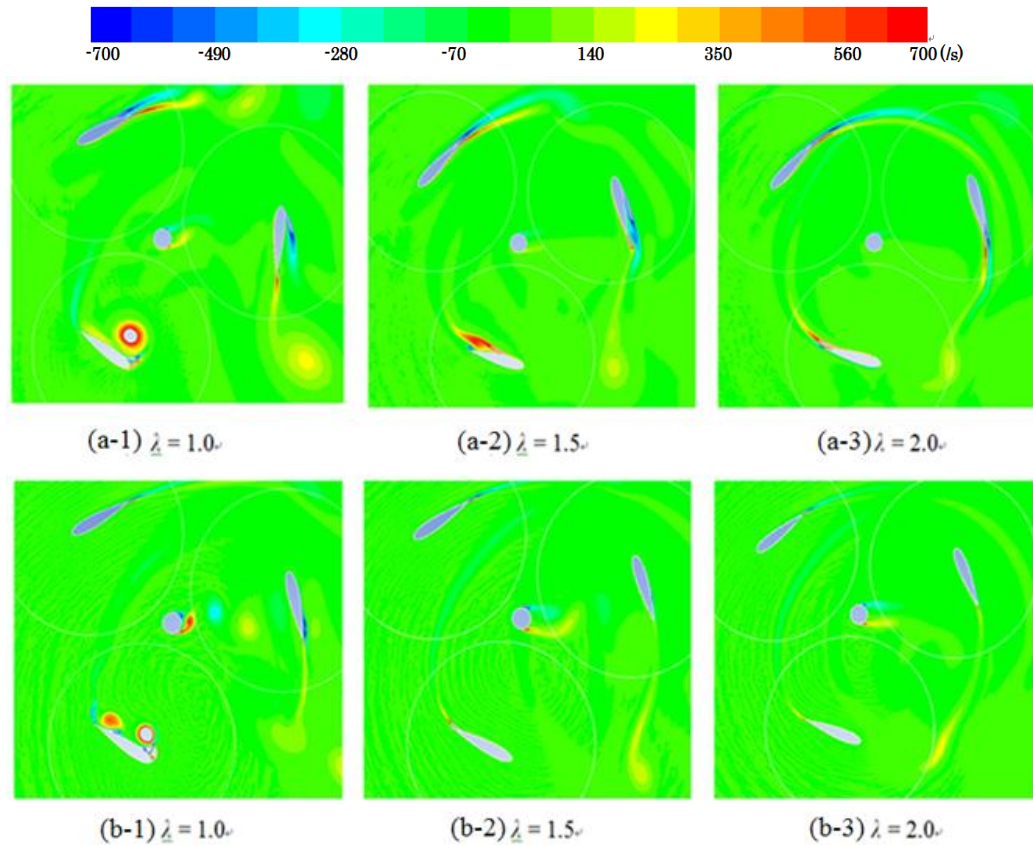


Fig. 8 Vorticity contours around the VAWT with fixed and variable-pitch blade (SST $k-\omega$ model, a. $\alpha_w = \pm 0^\circ$ b. $\alpha_w = \pm 10.2^\circ$)

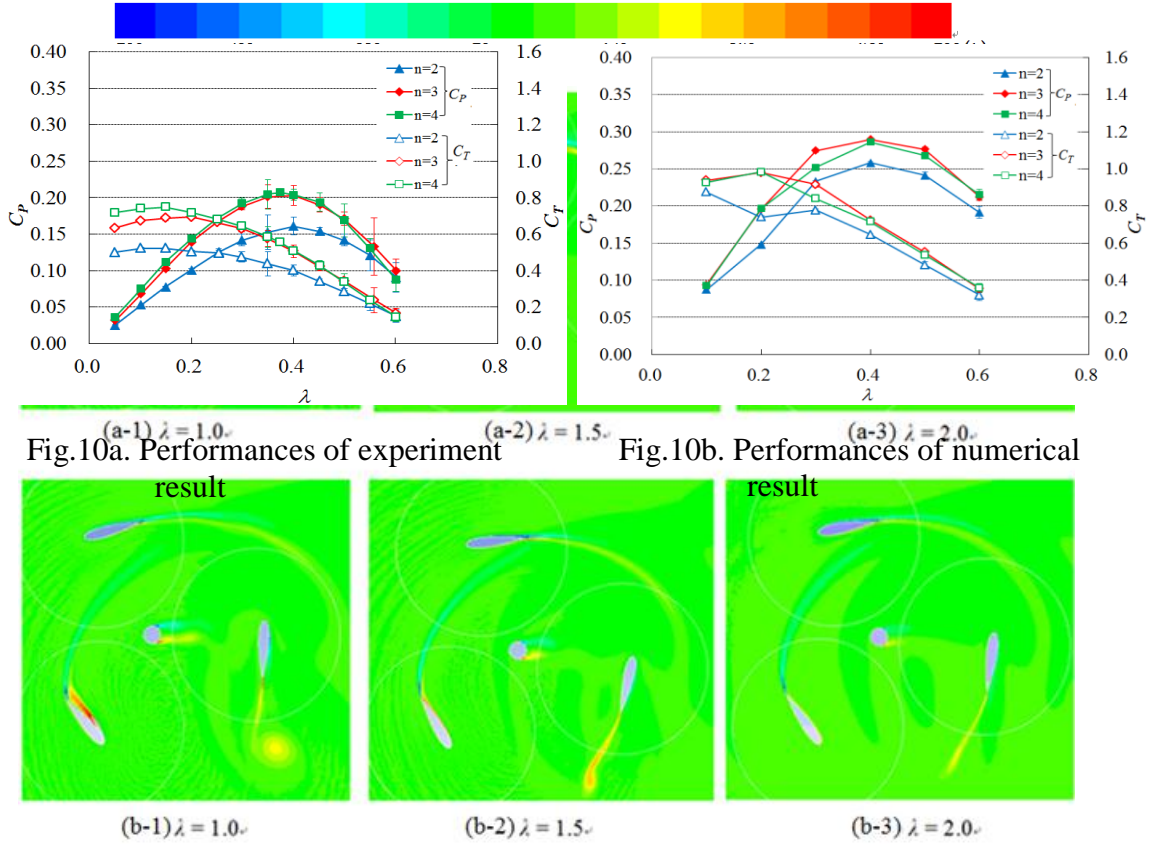


Fig.10a. Performances of experiment

Fig.10b. Performances of numerical

Fig. 9 Vorticity contours around the VAWT with fixed and variable-pitch blade (RNG $k-\varepsilon$ model, a. $\alpha_w = \pm 0^\circ$ b. $\alpha_w = \pm 10.2^\circ$)

On the other hand, Fig. 8(a) and Fig. 9(a) show the presence of a vortex on fixed-pitch blades with $\alpha_w = \pm 0^\circ$ for a TSR of $\lambda = 1.5$. The difference between the presence and absence of vortices at the same TSR for variable- and fixed-pitch blades is due to the amplitude and the rate of increase of the angle of attack. The numerical simulation using the SST $k-\omega$ model can predict as well as dynamic stall phenomenon which presence of vorticity behaviour on the rotor blade.

3.2 The Orthopter wind turbine

3.2.1 Power and torque coefficient of experiment and numerical results

The prediction power and torque coefficient of numerical results have good agreement with experiment results. The influences of number of blades of rotor and tip speed ratio corresponding to the coefficient performance and torque coefficient as seen in Figs 10a and 10b. The highest performance is the rotors which have three and four blades compared to the rotor have two blades. The peak of coefficient performance for the rotor have two, three, and four blades occur at $\lambda \approx 0.4$ which the rotor have two blades, the peak of performance coefficient shift to right slightly as seen in figure 10a.

3.2.2 Effect of aspect ratio and tip speed ratio on performance

The orthopter wind turbine has different of torque generation compare the other model wind turbine. Torque generated start from azimuth angle $\theta = 120^\circ$ until $\theta = 360^\circ$ due to combination lift type and drag type on power generation. The effect of aspect ratio on the power coefficient is shown in figure 11. The highest performance

for three blades rotor has aspect ratio $AR = 1$. Figure 12 showed tip speed ratio effect on the torque coefficient in one blade. The differences of torque coefficient especially at azimuthal angle between $\theta = 240^\circ$ and $\theta = 330^\circ$.

3.2.3 Effect of blade number on performance at different tip speed ratio

The effect of blade number on torque coefficient at different tip speed ratios are shown in Figs 13 and 14. Figure 13 showed effect blade number at low tip speed ratio which, the rotor with 2 blade has higher torque coefficient followed by rotor with $n=3$ and $n=4$ blade. However, the different torque for $n=2$, $n=3$, and $n=4$ at high tip speed ratio slightly decrease compare to low tip speed ratio. The different torque generated at low and high tip speed ratio for different blade number due to flow interference between blade which, lead to pressure coefficient between suction and pressure side

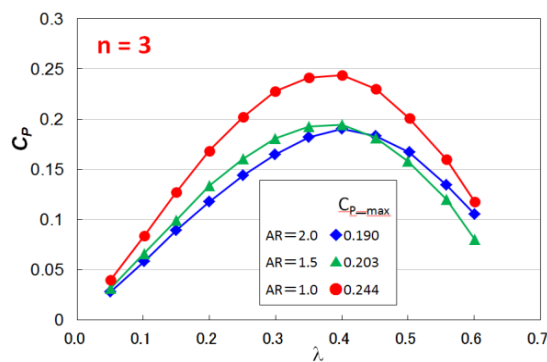


Fig.11. Performances of experiment result

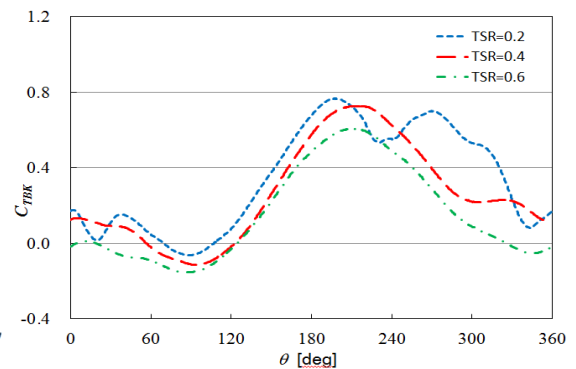


Fig.12. Effect tip speed ratio on torque coefficient for $n = 3$

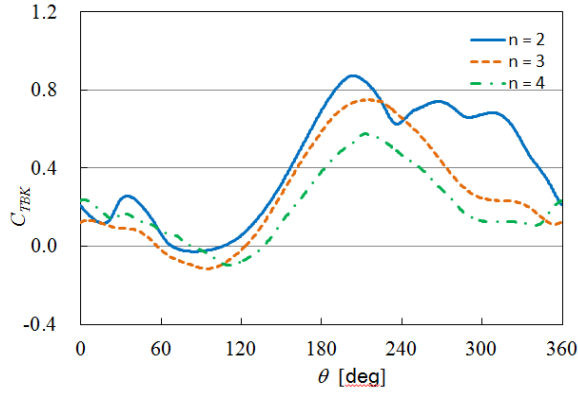


Fig. 13 Effect of number of blade on torque coefficients for $\lambda = 0.4$

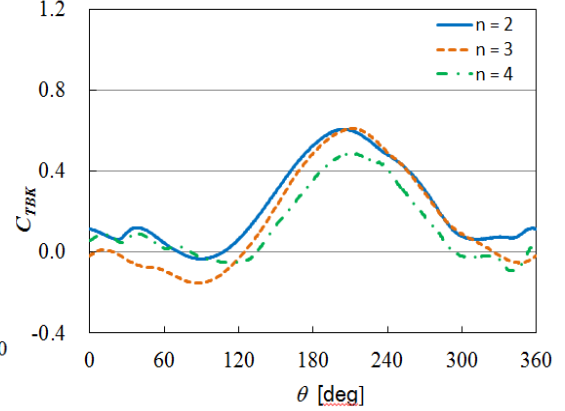


Fig. 14 Effect of number of blade on torque coefficients for $\lambda = 0.6$

4. Conclusions

The effects of the variable pitch angle, TSR, and turbulent model on the performance of a Darrieus wind turbine and the unsteady flow around the blades was investigated using a two-dimensional numerical simulation. The numerical simulation of the power performance results were validated using wind tunnel experimental data. The following conclusions were drawn:

- (1) The prediction of performance by numerical simulation using the RNG $k-\varepsilon$ turbulence model qualitatively agreed with the experiment. It was found that a VAWT with variable-pitch blades has better performance than a VAWT with fixed-pitch blades.
- (2) The performance of a VAWT is influenced by the amplitude and the rate of increase of the angle of attack. Reducing the angle of attack improves the torque coefficient, especially in the upwind area and some areas downstream, where a positive torque is generated on the VAWT with variable-pitch blades.
- (3) For a low TSR of $\lambda < 1.5$ in a VAWT with variable-pitch blades, positive power is generated in both the upstream and downstream areas. For a high TSR of $\lambda > 1.5$, the downstream power coefficient becomes negative, and the power coefficient decreases as the TSR increases.
- (4) The RNG $k-\varepsilon$ turbulence model can capture the presence of a vortex on the blade rotor at low TSRs. A VAWT with variable-pitch blades can significantly suppressed the leading and trailing-edge separation as compared to a VAWT with fixed-pitch blades.

The effects of aspect ratio, TSR, and number of blade on the performance of the Orthopter were investigated by wind tunnel experiment and the unsteady flow around the blades and predict performance influences by TSR and number of blade were investigated using a two-dimensional numerical simulation. The following conclusions can be reveals;

1. The performance of the orthopter influenced by aspect ratio, which the highest performance is the rotor has $AR = 1$

2. The prediction of performance by numerical simulation using the RNG $k-\varepsilon$ turbulence model qualitatively agrees with the experiment. It was found that the performance affected by number of blades and tip speed ratios.
3. The high tip speed ratio lead to reducing torque generation specially at downstream area
4. The simulations show effects of number of blade on the performance. The high number of blade reduces torque generation of one blade. However, the overall of performance is increased

学位論文審査報告書（甲）

1. 学位論文題目（外国語の場合は和訳を付けること。）

Numerical and Experimental Studies of a Small Vertical-Axis Wind Turbine with
Variable-Pitch Blades (可変ピッチ翼を有する小形垂直軸風車の数値及び実験的研究)

2. 論文提出者 (1) 所 属 システム創成科学専攻

(2) 氏 名 ラチマト フィルダウス
Rachmat Firdaus

3. 審査結果の要旨（600～650字）

当該学位論文に関し、平成27年1月27日9時45分より第1回学位論文審査委員会を開催し、提出された学位論文及び関係資料に基づき内容を検討した。さらに同日11時00分より口頭発表を行い、発表後に第2回学位論文審査委員会を開催し、協議の結果、以下の通り判定した。

申請論文は、2～4枚の直線翼を有する風車が回転しながら翼が独立して揺動運動する可変ピッチ式のストレートダリウス風車とオルソプタ風車の小形垂直軸風車の性能を数値解析と風洞実験で調べたものである。ストレートダリウス風車に関して、乱流モデルが風車出力の予測に及ぼす影響や、トルクが増減する回転角度と流れ場の関係を汎用熱流体解析コードのANSYS FLUENTによる数値解析で示し、最適な揺動角度の作動条件を風洞実験からも明らかにした。さらに、オルソプタ風車に関して、平板翼の枚数やアスペクト比を変化させて風車出力が最大となるソリディティ値を見出し、トルクが増減する回転角度と流れ場との関係を明らかにした。

以上のように、本論文は、可変ピッチ式小形垂直軸風車周りの流れ場と性能向上に関する有用なデータを示した研究であり、関連する風力エネルギー分野に寄与するところが大きいと判定し、博士(工学)に値するものと認定した。

4. 審査結果 (1) 判 定 (いずれかに○印) 合 格・ 不合格

(2) 授与学位 博 士 (工 学)